CRS4 Internal Report

Centre for Advanced Studies, Research
and Development in Sardinia
Pula (CA) - Italy

CRS4-PEC

Extensions of the SSTF model for applications in which density depends on temperature

VERSION 1.0
January 22, 2008

Prepared by:

V. Moreau
"Energy & Environment" program

Abstract

This paper is devoted to premixed combustion modelling in turbulent flow. First, we briefly give the main features of the SSTF model and its shortcomings, more extensively developped in a former paper. Then, we carefully describe some improvement of the model. The turbulent flame velocity is based on the observed self-similarity of the turbulent flame and uses the local flame brush width as a fundamental parameter, which must be retreived. We derive more rigorously the way density variations have to be taken into account in the width retreiving fuction. We reformulate the diffusion term as a classical flux divergence. We enforce the compatibility of the model for the limit of small turbulence. We include a contracting effect of the source term, allowing to give a stationnary monodimensional asymptotic solution with finite width. We also include in a preliminary form, a stretch factor, which proves to be useful for controling the flame behaviour close to the flame holder and near the walls. The model implementation in the StarCD CFD code is then tested on three different flame configuration. Finally we shortly discuss the model improvements and the simulation results.

Contents

1 Introduction

This paper is dedicated to a proper extension, taking into account additional features, of the Self Similar Turbulent Flame (SSTF) model to multi-dimensional cases, its integration for CFD analysis and its validation, in the framework of premixed turbulent combustion. We use the same formalism as for the Turbulent Flame Closure (TFC) model [1] and use the same structure of the mean progress variable equation $\tilde{c}$. The model construction is therefore reduced to the finding of an appropriate propagation velocity and a suitable diffusion-like term. Lipatnikov and Chomiak [2], from an extensive analysis of experimental data, have clearly put in evidence that the flame brush has a strong self-similarity property as a function of the mean progress variable. The model proposed is constructed on this property. In fact, we invert the classical approach in which the self-similarity is checked a posteriori to validate the model. The SSTF model main peculiarity is the introduction of the flame brush width as a fundamental parameter of the problem and the demonstration that it can be effectively used. Nevertheless, the former version of the model had two major drawbacks. First, the effect of the density variation due to the temperature was taken into account on a completely empirical manner. Second, the velocity-based diffusion term was not by force of integral zero, which is a rather large drawback for a diffusion term. In the following, we show how we solve this two defects. Then we introduce a contracting effect of the source term, enforcing the model compatibility with an asymptotical stationary mono-dimensional flame brush behaviour with finite width. We also modify the source term to have a consistent behaviour in the limit of small turbulence and introduce a strech factor which helps control some flash-back phenomena (be it of numerical, modelling or physical nature) near the flame holder and close to the walls.

2 Modelling Basis

We present here shortly the basis at the origin of the SSTF model.

In premixed turbulent combustion, the turbulent flame brush exhibits strong self-similarity features [2]. It is now known to be locally made of a highly corrugated flamelet sheet. In our study, we will suppose that the flame brush characteristics depend on the unstrained laminar flamelet parameters, on the turbulence parameters and eventually on time. We will use the "l" subscript for the laminar flamelet parameters and the "t" suscript for the turbubent brush parameters. For turbulence, the self-similarity parameter, according to Kolmogorov's theory is the energy dissipation ϵ. Lami-

nar flamelets gives small scale parameters and should not influence the flame brush self-similarity dimensionality. Moreover, we hope (and will suppose) that the laminar flamelet behaviour will influence the flame brush characteristics only through one unique combination of fundamental parameters. Therefore, $\epsilon_t = \frac{U_t^3}{\delta_t}$, where U_t and δ_t are the flame brush velocity and width, is a good a priori choice. It is associated with the laminar flamelet parameter $\epsilon_l = \frac{S_l^3}{\delta_l} = \frac{S_l^4}{\chi}$ where S_l is the laminar flame speed, δ_l, its width and χ the gas diffusion. If ϵ_t is a self-similar parameter, then one of its simpliest functional dependence on turbulence and laminar flamelet parameters is the following:

$$\epsilon_t = \epsilon^a \cdot \epsilon_l^{1-a}. \tag{1}$$

There is no explicit time dependance in the former expression because the self-similarity property is time invariant. We expect the coefficient a to be close to $\frac{1}{2}$ for various reasons given elsewhere [3], so from now on, we consider $a = \frac{1}{2}$. The flame brush has a very clearly defined front. Its width is therefore better described by the distance δ_t between the boundary rather than by the mean dispertion. Clearly, thanks to the self similarity property, the two approaches give proportional results. So, we will address the brush width evolution having in mind the evolution of its forward and backward fronts. By analogy with classical turbulent diffusion propagation with front, we will consider that the enlargement speed is proportional to the turbulent pulsation. As the width seems to be convected by the combined effect of the main flow and of the brush velocity, we arrive to the following simbolic representation:

$$\partial_t \delta_t + (u + U_t \cdot n) \cdot \nabla \delta_t = u', \tag{2}$$

where u' is the turbulent velocity pulsation and $U_t \cdot n$ the brush velocity.

In synthesis, our model is:

$$\epsilon_t = \epsilon^{0.5} \cdot \epsilon_l^{0.5}, \tag{3}$$

$$\partial_t \delta_t + (u + U_t \cdot n) \cdot \nabla \delta_t = u'. \tag{4}$$

We note that, in the case of anchored flames, the modulus of the convecting velocity decreases with increasing brush velocity. Therefore, for a given distance from the flame holder, the brush has more time to increase. The model predicts therefore an increase of the brush width when the flame brush velocity increases.

To implement this model in a CFD code, one must be able to evaluate locally δ_t. This is done using the self-similarity of the flame brush and choosing a reasonable shape. The local value of δ_t can in this way be retrieved from the local value of $\tilde{c}$ and $|\nabla \tilde{c}|$. In effect, stating the self-similarity of the flame is

saying : $c = f(x/\delta)$ and by differentiation $\delta = \frac{f'(x/\delta)}{\partial_x c}$. This last expression is then adapted to multidimensional cases. The function f is chosen a priori. As the brush width is retreived from the progress variable, we do not use its equation. The behaviour described by equation 4 can be implemented through the introduction in the mean progress variable equation of a diffusion velocity U_{diff} whose value depends on $\tilde{c}$ and compatibly with the shape choice. To be compatible with equation 4, we take $U_{diff} = f^{-1}(\tilde{c})u'$. The second order classical diffusion term of the $\tilde{c}$-equation is then replaced by $\overline{\rho}U_{diff}|\nabla\tilde{c}|$.

This methodology allows in principle to generate a diffusion region with a finite front velocity. And this velocity can be made dependent on the diffusion layer width.

Two order one constants A and B are introduced in the CFD model to fit the experiment. Finally, we have:

$$U_t = A\delta_t^{\frac{1}{3}}\epsilon^{\frac{1}{6}} \cdot \epsilon_l^{\frac{1}{6}}, \quad (5)$$

$$\text{“}[\nabla \cdot D_t \nabla\tilde{c}]'' = B\overline{\rho}U_{diff}|\nabla\tilde{c}|. \quad (6)$$

The mean progress variable equation that was implemented is therefore:

$$\partial_t\bar{\rho}\tilde{c} + \nabla \cdot \bar{\rho}\tilde{u}\tilde{c} = B\overline{\rho}U_{diff}|\nabla\tilde{c}| + \rho_u U_t|\nabla\tilde{c}|. \quad (7)$$

From a practical point of view, we have used the following function family to get back the brush width:

$$\delta = [\frac{\sqrt{\rho_u\rho_b}}{\bar{\rho}}]^a \frac{[\tilde{c}(1-\tilde{c})]^b}{|\nabla\tilde{c}|} \quad (8)$$

with a and b between 0.5 and 1.

This modelling has been implemented in the Star-CD commercial CFD software through user routine programming and numerical results have been presented in [3].

Nevertheless, the RHS term in equation 6 is not satisfying because it is not a pure diffusion term, not being by force of null integral. Moreover, the arbitrariness of the"δ" retrieving function is really excessive, mainly for what concerns the density dependency.

3 Modelling improvement

3.1 Basics

The original unclosed progress variable equation reads:

$$\partial_t \overline{\rho c} + \nabla \cdot \overline{\rho} \tilde{u} \tilde{c} = \overline{\dot{S}} - \nabla \cdot \overline{\rho} \widetilde{u" c"} \tag{9}$$

takink into account that $\rho_b \bar{c} = \bar{\rho} \tilde{c}$, where ρ_b is the (constant) density of the burned mixture, and defining S by $\rho_b S = \overline{\dot{S}} - \overline{\rho} \widetilde{u" c"}$, equation 9 can rewritten as:

$$\partial_t \bar{c} + \nabla \cdot (\tilde{u} \bar{c}) = S. \tag{10}$$

Taking into account that $\tilde{c}$ is function of ρ, one can combine the mass equation and equation 9 to eliminate the time derivative term. One gets:

$$\nabla \cdot \tilde{u} = (1 - \frac{\rho_b}{\rho_u}) S. \tag{11}$$

To address the density consistency problem, we now turn to the classical mono-dimensional case for which equation 11 can be integrated, giving:

$$\tilde{u} = u_0 + (1 - \frac{\rho_b}{\rho_u}) \int_{-\infty}^{x} S. \tag{12}$$

We seach a self-similar solution for which S has the functional form:

$$S = u_0 \partial_x F(\bar{c}, \delta) \tag{13}$$

where δ is a non better defined length depending only on time and having vocation to become the self-similarity parameter.

Inserting equation 13 in equation 10, one gets after some algebra:

$$\partial_t \bar{c} + u_0 \partial_x (\bar{c} - \frac{\bar{\rho}}{\rho_u} F(\bar{c}, \delta)) = 0. \tag{14}$$

We need to separate the functional dependances in $\bar{c}$ and δ, that is:

$$\bar{c} - \frac{\bar{\rho}}{\rho_u} F(\bar{c}, \delta)) = H(\delta) G(\bar{c}). \tag{15}$$

This can be done taking:

$$F(\bar{c}, \delta)) = \frac{\rho_u}{\bar{\rho}} [\bar{c} - \frac{u_1}{u_0} H(\delta) G(\bar{c})]. \tag{16}$$

Noting g the derivative of G ($g = G'$), we have:

$$\partial_t \bar{c} + u_1 H(\delta) g(\bar{c}) \partial_x \bar{c} = 0. \tag{17}$$

This last equation has a self-similar solution whose profile is the inverse of the function g.

Turning back to the original source term, with some additional algebra, we get for the monodimensional case:

$$\overline{\dot{S}} - \nabla \cdot \overline{\rho} \widetilde{u"c"} = \rho_u u_0 \partial_x \tilde{c} - u_1 H(\delta) \partial_x [\frac{\rho_u \rho_b}{\bar{\rho}} G(\bar{c})]. \tag{18}$$

As usual, we must stress the fact that there is no a priori one to one corrispondance between the tho left hand side and the two right hand side terms. Nevertheless, in the following will report the first RHS term as the "source" term Σ, and the second one as the "diffusion" term D.

A reasonable extension of the source term to the multidimensional case is:

$$\begin{aligned} \Sigma &= \rho_u U_t |\nabla \tilde{c}| & (19) \\ &= -\rho_u U_t n \cdot \nabla \tilde{c} & (20) \end{aligned}$$

where U_t is now the turbulent burning velocity and n is the normal vector defined by $n = -\frac{\nabla \tilde{c}}{|\nabla \tilde{c}|}$.

The function G is defined up to a constant. If we add a constant to G, as $\frac{1}{\bar{\rho}}$ is proportional to $\tilde{c}$, the constant part can be moved to the first RHS term in equation 18. Doing this, we are just stating that U_t can be dependent on δ.

In a former version of the SSTF model, the diffusion term was velocity based and was written as a classical convective transport term. Here, we will rewrite the monodimensional diffusion term such as to make naturally appear a divergence term more classical and natural for a diffusion effect. We have:

$$\begin{aligned} D &= -u_1 H(\delta) \partial_x [\frac{\rho_u \rho_b}{\bar{\rho}} G(\bar{c})] & (21) \\ &= \partial_x [u_1 H(\delta) \frac{\rho_u \rho_b}{\bar{\rho}} G(\bar{c}) n]. & (22) \end{aligned}$$

Here, $n = -1$ is the normal to the front for a fresh mixture at x negative: $n = -\frac{\partial_x \tilde{c}}{|\partial_x \tilde{c}|}$ or $n = -\frac{\partial_x \bar{c}}{|\partial_x \bar{c}|}$. In the turbulence context, the velocity u_1 should be strongly linked to the turbulent velocity pulsation u' and we have the following natural extension:

$$D = \nabla \cdot [u' H(\delta) \frac{\rho_u \rho_b}{\bar{\rho}} G(\bar{c}) n]. \tag{23}$$

An intersting particular case is when $H(\delta) = \frac{L}{\delta}$ where L is proportional to the integral length scale. Recalling that $\delta = \frac{1}{g'(\bar{c})|\nabla \bar{c}|}$, we have:

$$\begin{aligned} D &= \nabla \cdot [u' L g'(\bar{c}) G(\bar{c}) \frac{\rho_u \rho_b}{\bar{\rho}} \nabla \bar{c}] \\ &= \nabla \cdot [u' L g'(\bar{c}) G(\bar{c}) \bar{\rho} \nabla \tilde{c}] \\ &= \nabla \cdot [D_t g'(\bar{c}) G(\bar{c}) \bar{\rho} \nabla \tilde{c}] \end{aligned} \tag{24}$$

where D_t is proportional to the turbulent diffusion.

This means that when the profile is based on the error function (primitive of a Gaussian), then $g'G$ is constant. This is possible only if $G(0) = 0$. For other reasonable profiles, to have D_t bounded, it is necessary (but not sufficient) to have $G(0) = 0$. Consistently with the possible dependance of U_t on δ, we will now on always consider that $G(0) = 0$.

Equation 24 shows that our diffusion term is both i) a generalisation of the classical diffusion term because it is not restricted to the error function profile and to only one temporal behaviour, and also ii) a restriction of the classical diffusion term because it applies, as is, only to normalized front profiles.

One can remark that, while the progress variable equation is stated in term of the Favre variable, that is a mean weigthed by density, the profile is naturally set in term of the Reynolds variable, that is a mean weighted by the volume. This is more consistent with the feeling that diffusion is fundamentally an exchange of volumes with different concentrations. It is also clear that for self-similar profiles of finite length, if the $\tilde{c}-$profile is symmetrical, then the $\bar{c}-$ profile is not, and reciprocally. We will focus our attention to profiles which are symmetrical in term of the Reynolds variable.

In light of these considerations, we give an updated general representation form for the diffusion term:

$$D = \nabla \cdot [D_t \frac{H(\delta) G(\bar{c})}{L|\nabla \bar{c}|} \bar{\rho} \nabla \tilde{c}] \tag{25}$$

and if we introduce the turbulent flame Prandtl number

$$\sigma = -\frac{L|\nabla \bar{c}|}{H(\delta) G(\bar{c})} = \frac{L}{\delta H(\delta) g'(\bar{c}) G(\bar{c})} \tag{26}$$

we revert to the classical form

$$D = -\nabla \cdot [\frac{D_t}{\sigma} \bar{\rho} \nabla \tilde{c}]. \tag{27}$$

Now, we are faced with the problem of choosing a reasonable and practical profile. By reasonable, we mean quite regular (at least continuous derivative), monotonous, with only one inflexion point having a non zero finite slope. By

$x \in$	$[-\frac{\pi}{2}, \frac{\pi}{2}]$	$[-1, 1]$	$]-\infty, +\infty[$	$]-\infty, +\infty[$
f	$\frac{sin(x)+1}{2}$	$\frac{1+x\sqrt{2-x^2}}{2}$	$\frac{e^x}{1+e^x}$	$\frac{1+erf(x)}{2}$
g	$\arcsin(2c-1)$	$c^{0.5}-(1-c)^{0.5}$	$\ln(\frac{c}{1-c})$	–
g'	$\frac{1}{\sqrt{c(1-c)}}$	$\frac{c^{-0.5}+(1-c)^{-0.5}}{2}$	$\frac{1}{c(1-c)}$	–
G	$-\sqrt{c(1-c)}$ $+\frac{(2c-1)\arcsin(2c-1)-\frac{\pi}{2}}{2}$	$\frac{2}{3}[c^{1.5}+(1-c)^{1.5}-1]$	$c\ln c$ $+(1-c)\ln(1-c)$	–
$g'G$	1 $+\frac{(2c-1)\arcsin(2c-1)-\frac{\pi}{2}}{2\sqrt{c(1-c)}}$	$\frac{-1}{3}\sqrt{c(1-c)}$ $\times[2-\frac{1}{(1+c^{0.5})(1+(1-c)^{0.5})}]$	$\frac{c\ln c+(1-c)\ln(1-c)}{c(1-c)}$	$-C_1$
$g'G(0)$	0	0	$-\infty$	$-C_1$
$g'G(0.5)$	$1-\frac{\pi}{2}$	$-\frac{1+\sqrt{2}}{6}$	$-4\ln 2$	$-C_1$

Table 1: Tentative profile functions f with their inverse g, the primitive G and the derivative g' of the inverse. The exact value of C_1 is yet unknown but is strictly positive (about 1) and finite.

practical, we mean explicite, with explicite inverse (g) and explicite primitive of the inverse (G).

In table 1, we can see that if we want to have a non-standart self-similar evolution of the profile, we just do not know how to do it easily for an error function based profile. The exponential profile would have been an optimum candidate because it has the great property that the Reynolds and Favre profiles are identical, just shifted one from the other. Unfortunately, it gives for the standart diffusion time behaviour a diffusion coefficient that goes to infinity for $c = 0$ and $c = 1$. The sinusoidal and square root based profiles are both relatively acceptable. The square root based profile has the slight advantage that the product $-g'G$ can be put in a form that avoids indetermined ratio which always need to be carefully treated numerically. A minor drawback of these two profiles is that they are only C^1, because their curvature is discontinuous at $c = 0$ and $c = 1$. Looking forward to improve this regularity, we can see that if g' behaves like $c^{1/n-1}$ close to $c = 0$, then profile regularity is C^{n-1}. This constatation naturally leads to consider a profile such that:

$$g(c) = N(n)[c^{1/n} - (1-c)^{1/n}] \tag{28}$$

where the parameter n is greater than 2 and $N(n)$ is a normalisation factor such that $-g'G(1/2) = 1$. That is:

$$N(n) = \frac{\sqrt{n+1}}{2\sqrt{0.5^{1/n} - 0.5^{2/n}}}. \tag{29}$$

n	1	2	3	4	5	6
$\frac{\delta_{slope}}{\delta_{bound}}$	1	0.71	0.53	0.42	0.35	0.30

Table 2: Ratio ot the length based on the maximum slope to the length based on distance between the boundaries for different values of the parameter n

.

The case $n = 2$ is the one given in table 1. For n greater than 2, their is no practical explicite profile anymore. But, as the profile f is never explicitely used, it does not give rise to practical implementation problems.

Looking at the funcion $-g'G$ for different values of n, we can see that between $n = 2$ and $n = 6$, it looks very much like the function $[c(1-c)]^{1/n}$, seemingly tending to a flat profile for larger n. Unfortunately, for $n = 7$ and greater, the maximum is no more in $c = 0.5$ and the shape is no more convenient. This restrict the field of interesting values for n to integers (for convenience) between 2 and 6; or, if we want a continuous curvature, between 3 and 6. To help making this choice, we can look at the ratio between the length given by the effective width of the profile and the length based on the profile derivative in $x = 0$ or $c = 0.5$ for different n. These ratio are given in table 2.

$$\delta_{bound} = \quad g(1) - g(0) = \quad \sqrt{n+1}[0.5^{1/n} - 0.5^{2/n}] \tag{30}$$

$$\delta_{slope} = \qquad g'(0.5) = \qquad 2^{1-1/n}\frac{\sqrt{n+1}}{n}[0.5^{1/n} - 0.5^{2/n}] \tag{31}$$

gives

$$\delta_{slope} = \frac{2^{1-1/n}}{n}\delta_{bound}. \tag{32}$$

In the following will consider $n = 3$, which is the minimum integer giving a continuous curvature and giving a length ratio about 0.5 which seems reasonable. Higher values of n lead to stiffer functions maybe more difficult to handle while not giving consistant improvements.

3.2 Short time/width behaviour

We still have to decide on the shape of the function $H(\delta)$. From the standart turbulent diffusion theory, we have that a sharp front should enlarge at constant speed, while a diffuse front has an enlargement rate proportional to the inverse of its width. Taking the turbulent lenght scale as the reference scale, this means:

$$H(\delta) \sim 1 \text{ for } \delta \ll L \tag{33}$$

$$H(\delta) \sim \frac{L}{\delta} \text{ for } \delta > L. \tag{34}$$

This behaviour can be reproduced just by setting:

$$H(\delta) = \frac{1}{\sqrt{1 + (\frac{\delta}{L})^2}}. \tag{35}$$

Numerically, it is implemented using a "switch" parameter, say "Ini" (for Initial), with value one (on) or zero (off) and writting:

$$H(\delta) = \frac{1}{\sqrt{1 + Ini \cdot (\frac{\delta}{L})^2}}. \tag{36}$$

3.3 Contracting effect of the source term

In the specific case of reactive flows, the turbulent flame brush can be asked to have a maximum width due to a slight contractive effect of the real source term. For exemple, one can consider that the complessive contracting effect of the real source term is proportional both to S_l and to δ, or alternatively, proportional to S_l and independent of δ, remembering that this effect may not be perceived for a brush width of order L. As the complessive turbulent diffusion effect scales like D_t/δ, the combined diffusion term should go to zero when $S_l(\delta/L)^a$, with $a = 1$ or $a = 0$, is of order D_t/δ, and this independently of the modeling of the purely convective part by U_t of the source. Modelling separately the contracting effect of the real source term, for consistency, we should rewrite equation 23 and following with S_l instead of u' and with $H(\delta) = (\delta/L)^a$:

$$Cont = \nabla \cdot [S_l \frac{\delta^a G(\bar{c})}{L^a |\nabla \bar{c}|} \bar{\rho} \nabla \tilde{c}] \tag{37}$$

or

$$Cont = \nabla \cdot [C_f \bar{\rho} \nabla \tilde{c}] \tag{38}$$

$$C_f = \frac{S_l \delta^{1+a} g'(\bar{c}) G(\bar{c})}{L^a} \tag{39}$$

defining in this way the "flame contraction coefficient" C_f.

In the end, the turbulent flame diffusion coefficient D_f is:

$$D_f = \frac{D_t}{\sigma} - C_f. \tag{40}$$

The turbulent diffusion D_t is proportional to the turbulent viscosity, both being related through the Schmidt number Sch which value for reacting scalars is usually taken to $Sch = 0.7$. As our treatment (even without contracting term) essentially lowers the turbulent diffusion value, but was not intended to

modify its mean value, we take $Sch = 0.6$ to approximately compensate this effect.

Solving $D_f = 0$ in equation 40, we get the asymptotic brush width δ_∞ and the asymptotic flame brush velocity $U_{f\infty}$. Considering $H(\delta) = L/\delta$ for the diffusion term, the result is:

$$\delta_\infty = L(u'/S_l)^{1/(1+a)} \tag{41}$$

$$U_{f\infty} = u'(S_l/u')^{(3a+1)/6(1+a)}(L/\delta_l)^{1/6}. \tag{42}$$

This last expression can be expressed in term of the traditional adimensional numbers, the turbulent Reynolds number $Re_t = \frac{u'L}{S_l\delta_l}$, the Damköhler number $Da = \frac{L/u'}{\delta_l/S_l}$ and the Karlovitz number $Ka = (\frac{u'}{S_l})^2 Re^{-1/2}$.

$$U_{f\infty} = u'Da^{(2a+1)/6(1+a)}Re_t^{-a/6(1+a)} = u'Da^{1/6}Ka^{-a/3(1+a)}. \tag{43}$$

To keep a small contribution for the contractive term even for brush widths somewhat greater than the turbulent length scale, we will consider $a = 0$ in the following. That is:

$$C_f = S_l\delta g'(\bar{c})G(\bar{c}) \tag{44}$$

$$\delta_\infty = L(u'/S_l) \tag{45}$$

$$U_{f\infty} = u'(S_l/u')^{1/6}(L/\delta_l)^{1/6} = u'Da^{1/6}. \tag{46}$$

Note that these last considerations have generaly no practical effect on real flame modelling because there are apparently no known existing highly turbulent flame wide enough to critically feel the contracting effect. By the way, for a pure theoretical point of view, we provide the model with a stationary monodimentional solution. Moreover, we also get a sound limit both for δ and U_f, for exemple when the profile is highly disturbed close to the walls.

Another way to decide the asymptotic length, is to state that the asymptotic velocity is independent of the laminar flame properties, as in [4]. This directly leads to the following formula:

$$\delta_\infty = L(\epsilon/\epsilon_l)^{1/2} = (L \cdot \delta_l)^{1/2}(u'/S_l)^{3/2} \tag{47}$$

$$U_{f\infty} = u'. \tag{48}$$

This formula looks sound only for high ratio ϵ/ϵ_l which in turn is not very consistent with the idea of critical dissipation presented later on.

More generaly, the problem is that also U_f is likely to be also involved in the mechanism creating the contraction. A better attention paid to the

contractive effect is likely to lead to a different expression in a future model improvement.

If, by chance, in an hypotetical case, the contracting effect is a relevant feature, and due to changes in the turbulence parameters, the brush is larger than the asymptotic limit, then the diffusion term becomes negative. In this kind of cases, it may be wiser to incorporate the contracting effect into the source term, using equation 22 with $u_1 = -S_l$ to get:

$$Cont = S_l H(\delta)\rho_u\rho_b\partial_{\tilde{c}}\frac{G(\bar{c})}{\bar{\rho}}|\nabla\tilde{c}|. \tag{49}$$

In alternative, the contracting term can be split in two parts, one cancelling the diffusion term setting the diffusion coefficient (close) to zero, and the residual part added to the source term.

This approach, while not applied in this paper, shall be prefered for an eventual extension of the model in the framework of Large Eddy Simulation (LES). Moreover, requiring that the contractive effect scales naturally with the LES filter size should help better define the contractive term.

3.4 Low Reynolds Asymptotic behaviour

The SSTF model is thought primarily for highly turbulent flows whose turbulent pulsation is quite larger than the laminar flame velocity. And therefore, as is, the model has not a correct behaviour when turbulence becomes arbitrarily small. A simple way to remedy is to simply add the Laminar flame velocity to the turbulent part. To get eventually a smooth transition from one regime to the other, or not to overestimate the flame brush velocity when the laminar and the turbulent velocities are about the same, we combine both velocity through some exponent α to define the Low Reynolds turbulent Flame velocity in the following form:

$$U_{fLR} = \quad (U_f^\alpha + S_l^\alpha)^{1/\alpha}. \tag{50}$$

with α a priori close to the intervalle $[1, 2]$.

For numerical implementation, here also we use a switch parameter, say Lrab (from the subsection title), with value zero or one and writting:

$$U_{fLR} = \quad (U_f^\alpha + Lrab \cdot S_l^\alpha)^{1/\alpha}. \tag{51}$$

3.5 Wall treatment by quenching

For the mean progress variable, the boundary condition used in presence of a solid wall is the no flux condition, that is a zero gradient normal to the wall.

This condition is not satisfying because it is contradictory with the profile shape. The result is that the brush width is highly overestimated close to the walls and this may lead to the appearance, development and propagation of a spurious flame along these walls. A simple way to eliminate this spurious flame is to give an upper limit to the flame width. There are two relatively natural limits for the flame width. The first comes from the eventual theoretical estimation of the mono-dimensional stationary asyptotic width. The second, much more prosaic, limit is to state that the brush width cannot be larger than the available space. Anyway, whatever reasonable limiting criteria should remove this problem without other effects on the simulation. In practice, this procedure is not always sufficient to prevent the flame to rise back along the wall. When the flow has time to develop, the turbulent dissipation tends to be very high along the wall, several order higher than the dissipation in the mean flow. Therefore, the flame burning velocity is also quite large there, due to its functional dependency. Looking for a sound criteria to limit this velocity, we found out that we neglected any possible stretch induced local extinction effect. In [5], the problem has been treated introducing a critical dissipation ϵ_{crit} proportional to the flame dissipation ϵ_l with a quite large proportionality coefficient. When the turbulent dissipation increases up to order ϵ_{crit} there is an increasing probability to have the flame locally quenched, and therefore the flame velocity must be correspondingly damped. Following the same argument, we will replace the turbulent dissipation by an effective (or damped) turbulent dissipation ϵ_{eff} in the definition of the flame brush velocity. We set:

$$\epsilon_{eff} = \frac{\epsilon}{(1 + \frac{\epsilon^2}{\epsilon_{crit}^2})^{3/2}} \tag{52}$$

$$\epsilon_{crit} = B^2 \cdot 15\epsilon_l \tag{53}$$

$$\tag{54}$$

with B about 2 from first preliminary simulations. The exponent 3/2 at the denominator is chosen so that the perturbation acts at power 1/2 in the source term. In case one uses the Low Reynolds variant, it is wiser to damp also the laminar part.

The quite high coefficient (corresponding also to $B = 2$ in the cited paper) can be justified by the extremely high intermittency of the real dissipation. While for the applications shown hereafter, this features is used to get rid of wall boundary problems, a closer attention in the future could give the possibility to effectively simulate some flash-back phenomena.

3.6 Source overshot

From the numerical point of view, the source term in the progress variable equation is not a transport term and is not constrained by some maximum principle. The result is that close to the burned flame brush boundary, mainly when the brush is very sharp, the progress variable overcomes unity at the end of each algorithm iteration. While the value is reset to unity at the begining of each iteration, the profile is modified and reaches unity with a not so small slope, leading to an apparent local brush width extremely sharp. As the source term depends on the width, it is locally lowered by this mechanism, and in some way the overshoot is self-controled. This may be however a concern for the diffusion which goes to zero in the cell concerned, if one uses the diffusion control for small brush width. One can limit the smalest value of the apparent width, for example to the laminar flame width or the the computational cell width. Some tests (not shown here) have shown that there is no substantial change, except for the automatic scale displayed when visualising the sharpness field (the inverse width field).

4 Numerical results

In the following, we show some simulation performed using the updated Self-Similar Turbulent Flame (SSTF) model. The numerical test cases are the same as the one presented for the preliminary version of the SSTF model. The first series of simulation is based on a V-shaped flame and is compared with visual experimental data given in [6]. The second test case is based on a Volvo experimental facility. The flame is maintained by a central triangular flame holder. The simulation is based on the one presented earlier and based also on input data given in [7]. The third test case is the Moreau burner as reported in [9] and [8].

Unless otherwise precised, the simulations have been performed with the following parameters:

- $g(c) = N(3)[c^{1/3} - (1-c)^{1/3}]$ (that is $n = 3$ in equation 28)
- The width is defined by $\delta = \frac{2}{g'(\bar{c})|\nabla \bar{c}|}$ and is limited by the asymptotic length
- $H(\delta) = \frac{L}{\delta}$ that is $\frac{1}{\sigma} = g'(\bar{c})G(\bar{c})$ in equation 27
- $a = 0$ in equation 37, that is $C_f = S_l \delta g'(\bar{c})G(\bar{c})$ and the contracting term is effective
- $\alpha = 2$ in equation 50, that is $U_{fLR} = (U_f^2 + S_l^2)^{1/2}$.
- $B = 2$ in equation 54 and ϵ_{eff} is effectively used.

- $A = 0.6$, in equation 6, that is $U_f = 0.6\delta^{1/3}\epsilon_l^{1/3}\epsilon^{1/3}$
- In the end, the source term is: $S = \rho_u(\frac{S_l^2+0.7^2\delta^{2/3}\epsilon_l^{2/3}\epsilon^{2/3}}{1+(\frac{\epsilon}{60\epsilon_l})^2})^{\frac{1}{2}}|\nabla\tilde{c}|$.

4.1 Turbulent premixed V-shaped flame

The SSTF model is compared with experimental data on an experimental test case performed by F. Dinkelacker and S. Holzler and described in [6]. This setup is neither really axial-symmetrical nor cartesian 2-dimensional. Differences in the simulations resulted to be quite marginal in former simulations and we present only cartesian 2-D simulations. Note that the constants A anf α of the SSTF model have been tuned precisely on this model. The model gives very good results compared with the experimental results. It gives the same global shape and the same tendency.

The mixture inlet is 2.5m/s in vertical at ambiant room temperature. The laminar veocities used in the simulations are respectively 0.19, 0.10 and 0.04 m/s and are not expected to be very accurate. The diffusion coefficient is taken equal to the air cinematic viscosity (Hypothesis of unit Lewis number), that is $1.57E-5m^2/s$.There is also a vertical co-flow at 0.5 m/s to avoid strong lateral boundary effects.

The experimental results are showed in figure 1. It is not totally clear what is the meaning of the figure, in terms of the calculated variable. Nevertheless, we will suppose that the apparent flame position is a good indicator of the progress variable. When dealing with visual observation, the weight averaging in the Favre-averaged progress is probably not taken into account. The Reynolds averaged progress variable seems therefore more adapted for confront, as is also considered in [6]. To evaluate the flame position, both variables are essentially shifted one another of a not so small fraction of the local brush width. In figure 2 and 3 we present the simulated profile respectively of the the Reynolds and Favre progress variable. In figure 2, we show the effect of the critical stress limitation which is almost non effective when B=2 (RHS), but moves the flame anchoring from under the flameholder to the lateral part of the flameholder when B=1 (LHS).

4.2 Volvo burner

This test case has been inspired from [7]. Parameters of the problem are: inlet velocity $18m/s$, turbulent intensity 3%, and length scale $8mm$. Molecular diffusivity $2.E-5m^2/s$, $A = 0.7$ laminar flame speed $0.743m/s$. Inlet temperature 600 K and burned temperature 1850 K. The flame holder is $4cm$ high in a rectangular channel 12 cm high and 24 cm wide. The problem can be

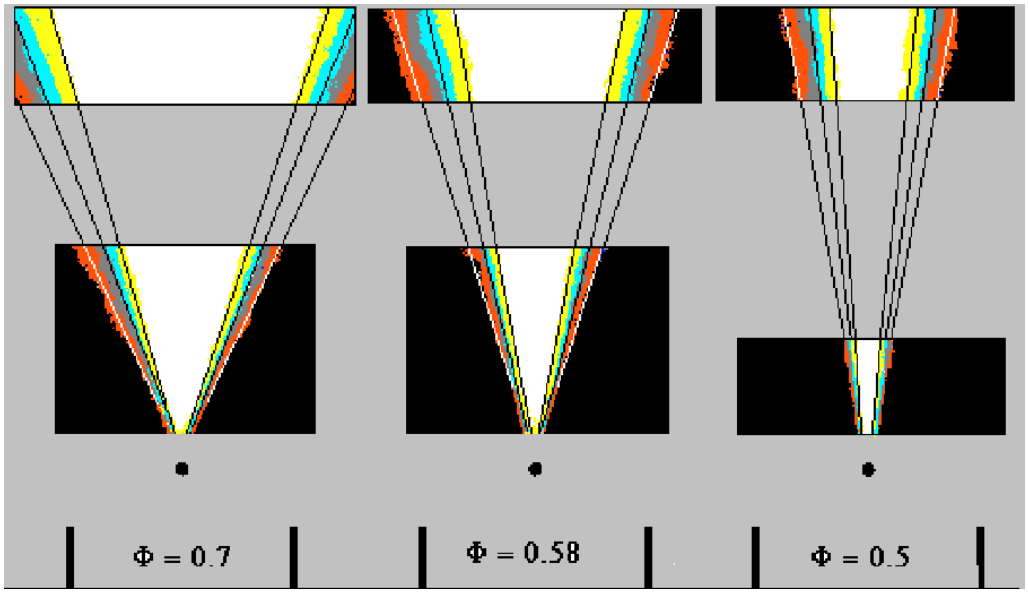

Figure 1: Experimental results: Soika, 1996; Dinkelacker, Holzler, Leipertz, 1999

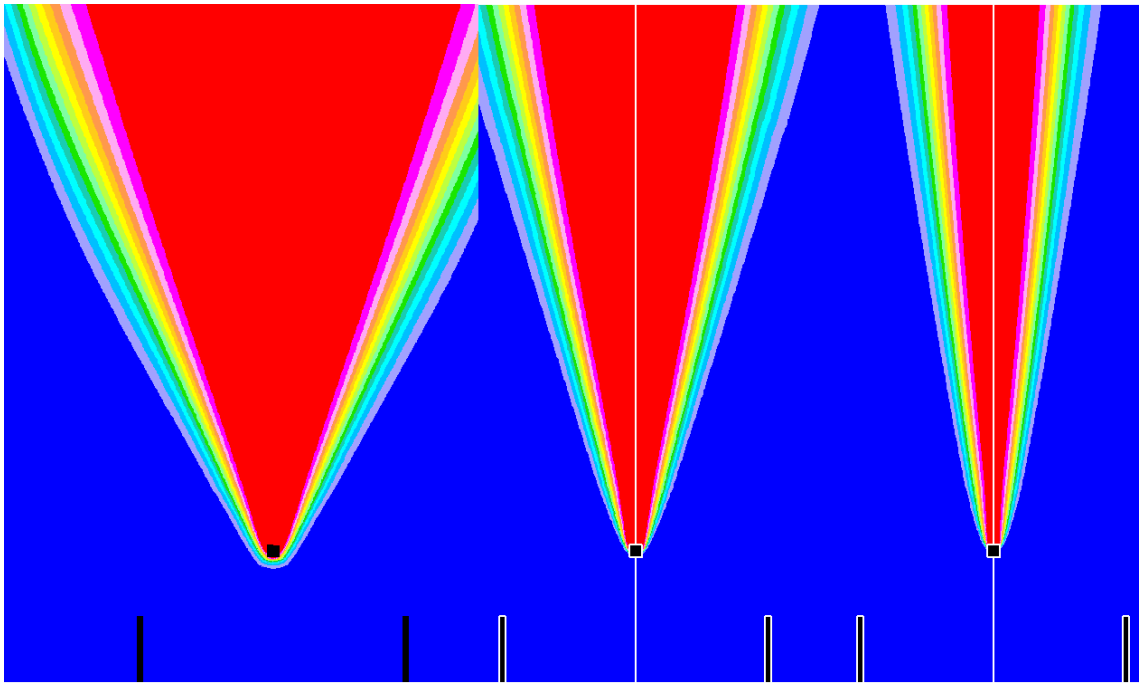

Figure 2: V-shaped flame. From left to right, the mean Reynolds averaged progress variable $\bar{c}$ for $\phi = 0.7$, $\phi = 0.58$ and $\phi = 0.5$. Parameters are: A=0.6 and B=2.

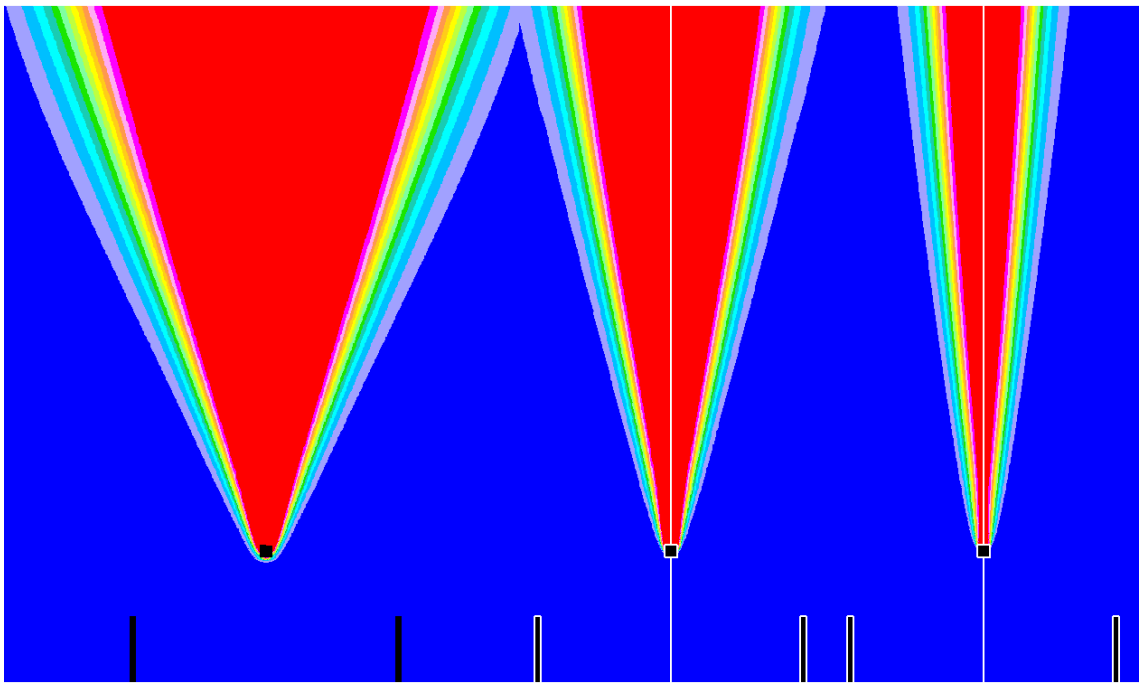

Figure 3: V-shaped flame. From left to right, the mean Favre averaged progress variable $\tilde{c}$ for $\phi = 0.7$, $\phi = 0.58$ and $\phi = 0.5$. Parameters are: A=0.6 and B=2.

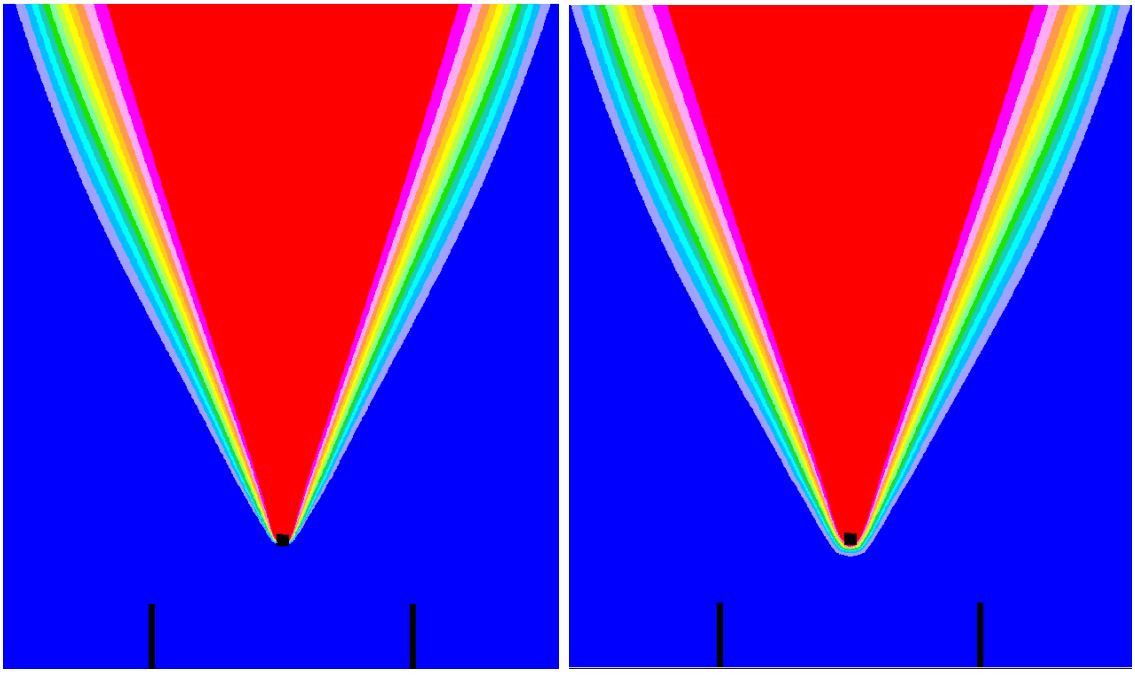

Figure 4: V-shaped flame. Mean Reynolds averaged progress variable $\bar{c}$ for $\phi = 0.7$ and A=0.6. On the LHS B=1 and on the RHS B=2.

reasonably rappresented 2-dimensional. The simulated domain extends up to 60 cm from the flame holder. In figure5, we show the Favre averaged progress variable in the given configuration (top) and with the parameter B changed from 2 to 4 (bottom). The difference can be seen near the walls close to the outlet. For the standard configuration, there is almost no flash-back effect, while the flash-back effect can be clearly seen when the stretch effect has been lowered.

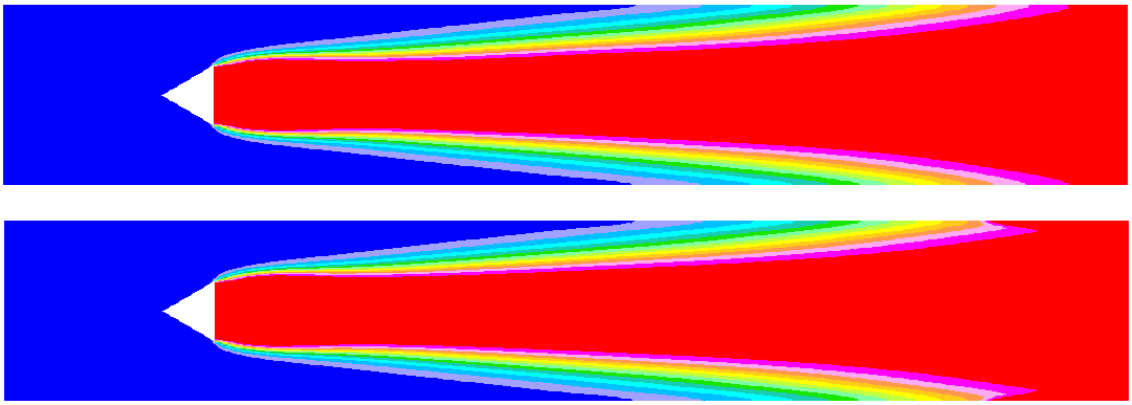

Figure 5: Favre Progress Variable for the Volvo burner Simulation. Upper, standard configuration, lower, parameter B controlling the stretch effect has been moved from 2 to 4.

The former parameters resulted, after control, unfit. The results should be interpreted only as a technical demonstration of feasibility. In[7], the inlet velocity is in fact about $34.1m/s$ and after control the diffusion coefficient is taken as $\chi = 5.27E^{-5}$. But the simulation resulted unstable with large oscillations and it was not possible to get a converged stationnary solution. This is illustrated in figure 6. Note that the presence of large Von Karman like vortices was noticed during the experiment as reported in [7]. So, it is normal not to have any stationary solution in the RANS framework. A stationary solution, obtained by simulating only one half of the domain wold be therefore strongly misleading.

4.3 Moreau burner

The simulation of the Moreau burner is taken from [9] and [8]. The inlet conditions are given in table 3. We used a laminar flame velocity of 1.15 m/s and a molecular diffusivity of $5.27E - 5m^2.s^{-1}$. The computational domain is 100 mm high for 1300 mm long, with 12500 cells.

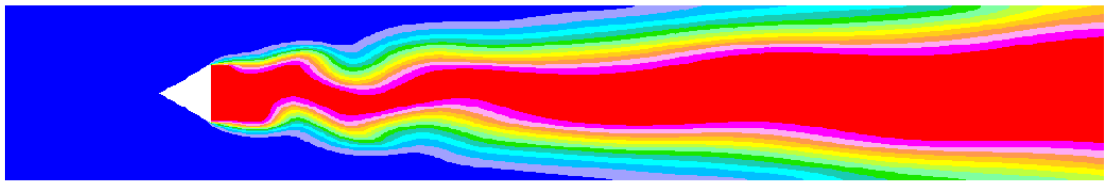

Figure 6: Favre Progress Variable for the Volvo burner Simulation. Inlet velocity 34.1 m/s, turbulence intensity 10%, $A = 0.6$. Transient, non converged simulation.

phase	T(K)	$\rho, kg.m^{-3}$	u (m/s)	u' (m/s)	$\kappa(m^2.s^{-2})$	$\epsilon(m^2.s^{-3})$	ϕ
burned	2240	0.1538	120	23	793	$2.8E6$	0.87
unburned	600	0.562	60	8	100	3.7E4	0.87

Table 3: Moreau burner test case. Inlet flow conditions for burned and unburned mixture

In figure 7, we show the progress variable in the computational domain. The top image has $B = 1$ while the bottom one has $B = 2$. The difference is very small and is concentrated close to the inlets junction. For $B = 1$, the combustion is slightly more delayed.

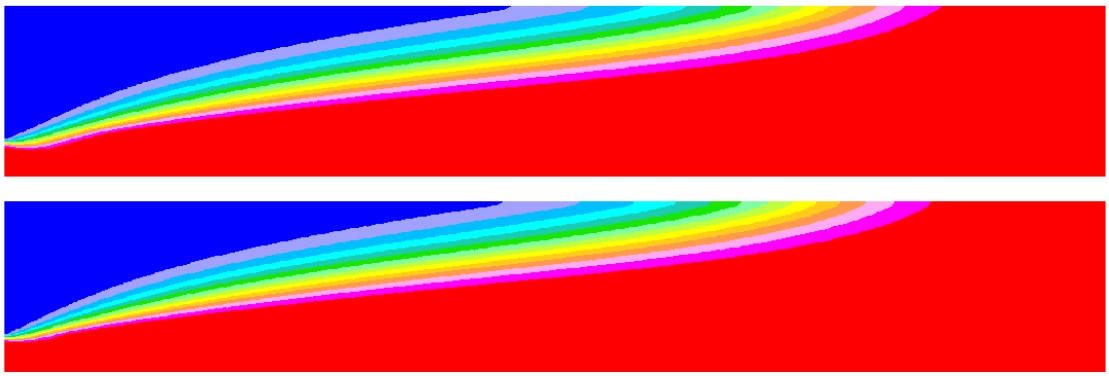

Figure 7: Moreau burner. TFC and standard $\kappa - \epsilon$ model. Progress variable. The flows enter from the left. Computational model is 100 mm high and 1300 mm long. Top picture, $B = 1$. Bottom picture, $B = 2$.

5 Discussion

In [3], we have proposed a turbulent flame brush model based on the Kolmogorov theory of turbulence and and the concept of self-similarity. By using a priori the concept of self-similarity of the flame brush width, we can retrieve locally a correct estimation of the brush width. Considering the reverse of the usual Taylor hypothesis on the equivalence of time and space dependence, we have in fact given access to the time dependence for modelling. As a side product, the self-similarity together with the access to the width allows to construct diffusion terms with non classical behaviour. First, the diffusion front can be made at finite velocity. Second, the diffusion can be made dependent on the width. This can be useful for exemple to model the initial part of the brush for which the standard diffusion theory gives a time dependence. These features can be introduced modifying the diffusion coefficient in the standard diffusion term. A drawback of the velocity based diffusion term was that, in the form proposed in [3], it was not neutral for the global consumption rate. Here, we have modified the form of the diffusion term so as to ensure that it is a pure diffusion one and put in the usual divergence form. By the way, in this paper, the alteration of the order of the diffusion term is not numerically investigated.

Another problem linked with the former version of the SSTF model was the effective width retrieving function. This function can be analytically found for very simple configurations in which there is no density change no shear and constant turbulent quantities. In this case, it depends on the expression used for the diffusion velocity term. Most problematic, was the density dependence that was implemented into the width retrieving function. This aspect is now largely clarified and the arbitrariness has been removed in the current model version.

The SSTF model has been derived mainly on the basis of the most simple assumption. A basic assumption is that the chemistry affects the model through only one parameter. This parameter is the “energy dissipation” for the SSTF model. In its original form, the SSTF model was not compatible with three asymptotic cases i) first, when the turbulent pulsation becomes the same order or smaller than the laminar flame velocity, ii) second, when the turbulence is so high than the flamelet structure completely disappears and iii) third, for the description of the academic stationary mono-dimensional behaviour.

The first asymptotic case is simply treated by adding the laminar flame velocity to the burning velocity through their square values, summing in fact their ”energetical strength”. This introduces the laminar flame speed as a

new chemical inependent parameter, which is against the basic asumption of only one chemical parameter. For now, we have to accept this "renuncement". The second asympotic case is treated through the introduction of a damping multiplicator of the source term, function only of the turbulent and "laminar" energy dissipation. So, we are still consistent with the assumption of only one parameter. The damping factor demonstrates to be very effective in controlling some flash-back phenomena in the Volvo-burner simulation, and the kind of attachment to the flame holder for the V-shaped flame. It deserves therefore much more attention and may be the object of future model development. The third asymptotic case is treated through the inclusion of a turbulent flame contracting (or anti-diffusive) effect. This effect is imbedded in the diffusion term in such a way that the diffusion vanishes when the asymptotic width is reached. Its implementation also helps to avoid absurd unbounded flame velocities near walls or some other potential pathological situation, in which a non trivial extrema or saddle-point (or "saddle-line in 3D) or the progress variable may appear. In the current implementation, the limiting width is based on an assumption which involves the appearance of the laminar flame speed as another "chemical" parameter, as for the first case. A greater care should be dedicated to this aspect and there are foreseenable changes in future model development.

There is still margin improvements for modelling into at least two directions:

- The damping of the diffusion when the brush width is very small is not yet tested. This has a direct effect on the local flame velocity because the flame brush erroneously enlarges too fast in the vicinicity of the flame holder or anchoring point. This aspect is of secondary importance for the evaluation of a priori stable flames (with no risk of blow-off). Nevertheless, it may become a critical point if we want to have some evaluation of the blow-off behaviour when it is linked to the detachment of the flame from the flame holder.
- The contracting effect of the turbulent flame must be generalized to perform even when it is greater than the turbulent diffusion. This is mainly a technical problem linked to the fact that the diffusion term in the CFD algorithm must absolutely be with a non-negative diffusion coefficient. Having a both way controlling term; that is a term able to effectively recontract the brush width seems to be an essential prerequisite to design a LES version of the model.

In [3], the fitting for the three cases considered lead to the parameter

A ranging from 0.5 to 0.9. The rationals and the improvements given to the model allow to perform again all the simulations with always the same constant $A = 0.6$.

6 Conclusion

We have included some improvements in a turbulent flame brush model based on self-similarity, simplechemistry coupling and Kolmogorov turbulent theory. The improved model has been implemented in the Star-CD commercial software and tested on three simulations where it gives very satisfying results. In this model, we consider that the brush width is a fundamental parameter which must be retreived. The density variation is now consistently taken into account, both in the width retreiving function and in the dissipation term. Several modifications have been included to be consistent with at least three asymptotic behaviours. The fitting constant A controling the local brush speed seems to be much less case dependent than in the former version of the model.

References

[1] V. Zimont F. Biagioli and K. Syed. Modeling turbulent premixed combustion in the intermediate steady propagation regime. *International Journal:Progress in Computational Fluid Dynamics*, Vol.1(Nos. 1/2/3):14–28, 2001.

[2] Lipatnikov A.N. and Chomiak J. Developing premixed turbulent flames: Part 1. a self-similar regime of flame propagation. *Combus. Sci. and Tech.*, 162:85–112, 2001.

[3] Moreau V. A self-similar turbulent flame model. *Applied Math. Modelling*, 2007. (In press).

[4] V. L. Zimont. Kolmogorov's legacy and turbulent premixed combustion modeling. In William J. Carey, editor, *New Devel. in Combustion Research*, chapter 1, pages 1,93. Nova Science, 2006. ISBN: 1-59454-826-9.

[5] Vladimir L. Zimont and Fernando Biagioli. Gradient , counter-gradient transport and their transition in turbulent premixed flames. In *Combustion Theory and Modeling*, volume vol. 6, pages 79–101. 2002.

[6] F. Dinkelacker and S. Holzer. Investigation of a turbulent flame speed closure approach for premixed flame calculations. In *Combustion, Science and Technology*, volume vol.158, pages 321–340. 2000.

[7] P. Nilsson and X.S. Bai. Effects of flame stretch and wrinkling on co formation in turbulent premixed combustion. In *Proceedings of the Combustion Institute*, number 29, 2002.

[8] Maciocco L. and Zimont V. L. Test of the tfs combustion model on high velocity premixed ch4-air combustion in a channel. In *20-th Annual Meeting of the Italian Section of the Combustion Institute*, pages X–2.1 – 2.4. Institute Frantic 97, 1997.

[9] V.L. Zimont M. Barbato and F. Murgia. On the limits of industrial premixed combustion simulation models. In *Mediterranean Combustion Symposium*. the Combustion Institute, June 20-25 1999.